

Magnetic Element Shape for Magnetic Random Access Memory (MRAM)

M. H. Park, Y. K. Hong,* S. H. Gee, and D. W. Erickson,
*Magnetic and Electronic Materials Lab., Department of Materials Science and Engineering,
University of Idaho, Moscow, Idaho 83844*

B. C. Choi
Department of Physics, University of Victoria, Victoria, British Columbia, Canada
C. A. Berven

Department of Physics, University of Idaho, Moscow, Idaho 83844

*E-mail: ykhong@uidaho.edu

Abstract

The results of magnetization configuration and switching behavior of sub-micron magnetic elements having various shapes are presented in this paper. The shapes include rectangle, hexagon, and Pac-man-like. Sputter deposition, e-beam patterning, and lift-off processes were used to fabricate an array of magnetic elements. Magnetic configuration and switching behavior of magnetic elements with various shapes were characterized by a magnetic force microscope. For the rectangular element, an unrepeatable switching behavior was observed due to magnetic defects involved during the magnetization reversal process and an array of hexagonal elements shows a wide switching field distribution. Both vortex and onion states are stable magnetization configurations in a ring element. An onion state becomes unstable with decreasing the ratio of inner to outer diameter of the ring and increasing thickness of the ring. On the other hand, a single domain was observed in the Pac-man element, while the modified Pac-man shows a bi-domain configuration. A reversal magnetization process in the modified Pac-man element is driven by the vortex core movement. An array of the Pac-man elements shows the highest switching field, but the narrowest switching field distribution as compared to rectangular and hexagonal elements of the same overall dimensions. Finally, We conclude the PM element has the most potential for a magnetic memory element in future MRAM devices.

1. Introduction

For decades, dynamic random access memory (DRAM) has completely fulfilled its role as computer memory. However, DRAM has to be refreshed about a hundred times per second to retain information on a huge capacitor built on a transistor, and the information even disappears whenever power is off. DRAM may not meet demands for future electronic memory devices because of

volatility, high power consumption, and difficulty in integration of capacitor at small feature size. Even though the huge market for non-volatile memory is currently occupied by the flash memories, a low writing speed, high writing voltage, limited endurance, and high fabrication cost will limit their future applications in non-volatile memory devices.

On the other hand, new types of non-volatile memory have been introduced. These non-volatile memories include ferroelectrics random access memory (FRAM) [1,2], Ovonic unified memory (OUM) [3,4], and magnetic random access memory (MRAM) [5,6], as summarized in table I. FRAM, which uses the polarity switching of ferroelectric materials by an electric field, shows a low power consumption and fewer mask processes than flash memory for integration with CMOS. However, FRAM has a fatigue problem and difficulty in high-density integration. In addition, the reading is a destructive process and the endurance is low. For OUM, a large resistance difference between the crystalline and amorphous phase of chalcogenides by quick electric heating is used to store information. This memory shows a low operation current and high compatibility with CMOS processes. However, OUM may be limited in some specific applications because of its low endurance and slow switching process. On the other hand, MRAM test devices show an almost unlimited endurance with a non-destructive read-write operation as well as a very fast access rate. Recent MRAM devices use two ferromagnetic films to sandwich an ultra-thin insulator, called a magnetic tunneling junction (MTJ). The MTJ is used as the memory component of MRAM. The information can be stored as "0" or "1" by the resistance difference in the MTJ's, which depends upon the magnetization direction of the two magnetic layers.

In order to successfully implement MTJ MRAM devices, there are several issues to address: repeatability of magnetization switching, uniformity of junction resistance over a 300 mm wafer size, and thermal stability of electric and magnetic properties up to 400 °C, which is compatible with the CMOS process. A prototype 256 kbit

MRAM test chip, with a variation of junction resistance less than 5 % over a 200 mm wafer, was fabricated by Motorola [7]. The insertion of a Fe-O layer between the barrier and free electrode layers of the MTJ improved thermal stability up to 380 °C [8]. However, the unrepeatable switching behavior of a submicron-sized magnetic element still remains as an obstacle to the densification of information data storage [9-12]. As a magnetic element size decreases to deep-submicron, the control of magnetic switching behavior becomes more difficult. This is attributed to lateral surface roughness caused by limited lithographic resolution [13-15].

In this paper, we present the results of magnetization configuration and switching behavior of sub-micron magnetic elements having various shapes and propose an optimized magnetic element shape for MRAM applications. The shapes in this study include rectangle, hexagon, and a new shape, called “Pac-man.” Arrays of sub-micron magnetic elements were prepared by electron beam lithography, sputter deposition and lift-off or ion milling processes. A scanning electron microscope (SEM), atomic force microscope (AFM), and magnetic force microscopy (MFM) were used to characterize the arrays of sub-micron magnetic elements.

2. Results and Discussion

2.1 Rectangle and hexagon elements

Most elements for magnetic random access memory (MRAM) devices have been linear in shape with modified ends such as a hexagon or an ellipse, not only because these are simple to pattern, but have shown much fewer magnetic defects such as edge domains [9], 360° domain walls [10], and localized vortices [11]. However, one of the most serious problems in the elements currently issued for commercialization of MRAM devices is a wide switching field distribution (SFD) due to the small end shape variation between elements caused by limited lithographic resolution. This problem can be compounded further when the element size decreases down to the deep-submicron. This is because the effect of lateral roughness on the demagnetizing field of a magnetic element is significant. A wide SFD should potentially have a higher risk for MRAM cells to fail since it provides a narrow margin of selectivity for these cells.

Figure 1 shows AFM and MFM images of a rectangular cobalt element of $0.5 \mu\text{m} \times 1.5 \mu\text{m}$ with a thickness of 32nm, observed at remanent state after saturating the element at 440 Oe and bringing it back to (b) 0, (c) -170, (d) -252, (e) -271, and (f) -331 Oe. Figure 1 (a) is an AFM image showing topology of the rectangular element. As shown in Figure 1, the magnetization configuration of the rectangular Co

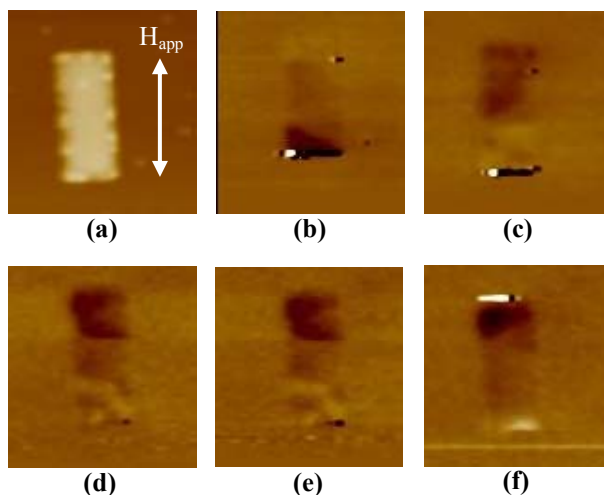


Figure 1. (a) AFM images of 32 nm thick Co rectangular element. MFM images at remanent state after saturating at 440 Oe, followed by a negative magnetic field of (b) 0 Oe, (c) 170 Oe, (d) 252 Oe, (e) 271 Oe, and (f) 331 Oe.

element at remanent state depends upon a previous switching history because of magnetic defects evolving during the switching process. Thus, the switching history dependence of magnetization configuration will result in switching field distribution of the magnetic element.

An array of 100 hexagonal permalloy elements with a dimension of $0.25 \mu\text{m} \times 0.75 \mu\text{m}$ with a thickness of 30 nm was scanned by a MFM to observe magnetic domain

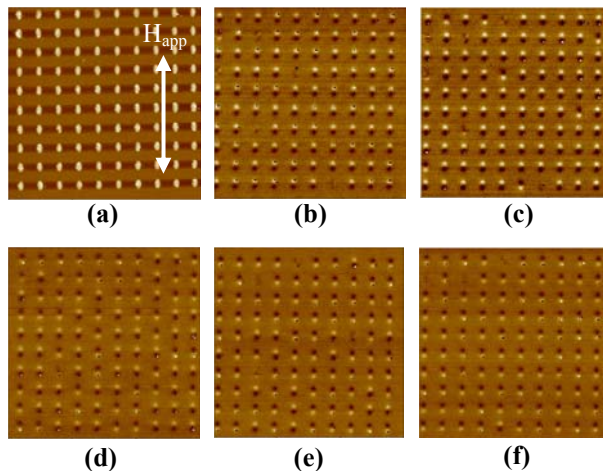


Figure 2. (a) AFM images of an array of 30 nm thick permalloy hexagonal elements. MFM images at remanent state after saturating at 440 Oe, followed by a negative magnetic field of (b) 60, (c) 100, (d) 150, (e) 180, and (f) 225 Oe.

configurations. Applied negative fields, prior to bringing the array to remanent state, were (b) -60 Oe, (c) -100 Oe, (d) -150 Oe, (e) -180 Oe, and (f) -225 Oe. As shown in Figure 2, even though an individual hexagonal element shows repeatable magnetic switching, the switching of an

array of hexagonal elements occurs in a wide range of applied fields from 60 Oe to 225 Oe. Magnetic charges built up at the sharp ends of the element align along the easy direction, consequently causing a high demagnetizing field along the easy direction. Therefore, a small change in the sharp end leads to a large change in the amount and direction of charges. Accordingly, a large variation in the demagnetizing field strength will result, leading to a wide SFD in the array of hexagonal elements.

2.2 Disk and ring elements

As an alternative, circular magnetic elements with vortex magnetization configurations, such as a disk [16,17] or ring [18,19] element, have been proposed for MRAM applications. According to micromagnetic computer simulation, a stable vortex magnetization configuration exists in the circular magnetic elements with an appropriate thickness [16,20]. Since it forms a closed magnetic domain, there is no magnetic charge at the edge of the element, thus no stray field. Therefore, the circular magnetic element would not show any localized vortex, 360° domain walls, or edge domains. In order to successfully implement the circular magnetic element for MRAM device applications, there is a need to switch magnetization not driven by a vortex core movement. This is because the vortex core in deep-submicron element makes a domain configuration unstable and the movement of the vortex core is a much slower switching process than coherent rotation. Thus, the disk-type element would not be a preferred choice for the MRAM device.

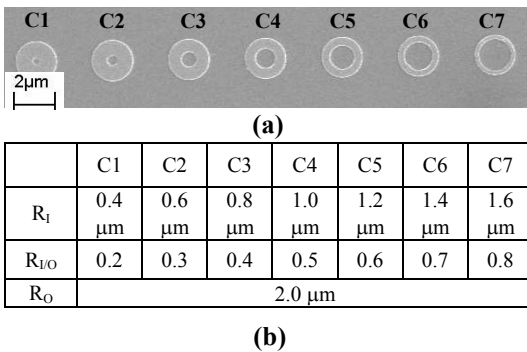


Figure 3. (a) SEM images of 40 nm thick permalloy ring elements and (b) the dimensions of the ring elements.

Instead, ring-shaped magnetic elements have gained interest for applications in magnetic memory devices due to their unique stable magnetization configurations.

Two stable vortex configurations, clockwise and counterclockwise vortices, have been known to exist in a ring element at remanent state, similar to disk elements. For MRAM applications, two stable vortices would be

used as two distinct bit states, 0 or 1. However, specially designed conducting wires are required, as suggested in a vertical MRAM structure [18], to achieve pure vortex switching. In order to avoid the complex wiring system, an idea on magnetic switching of ring elements by an in-plane magnetic field was sought. Thus, an asymmetric ring element was proposed by J. A. C. Bland et al. [19, 20] to meet the in-plane field switching. In this shape, magnetization reversal occurs by the motion of domain walls nucleated at a notch or naturally produced defect during the fabrication process. Recently, two stable magnetization configurations, namely “onion” states, were observed at remanent state in a narrow ring element [21]. The onion state has two symmetrical single domains with head-to-head (HTH) domain walls. A ring element with the onion state rather than the vortex state is more favorable for two-bit states in MRAM devices because it is easier to switch the onion state configuration by an in-plane applied field [21].

Scanning electron microscopy (SEM) images of permalloy ring elements are shown in Figure 3 (a), and the dimensions of the ring elements are detailed in Figure 3 (b). Figure 4 shows the MFM images of the permalloy ring elements with an outer diameter of 2 μm and a thickness of (a) 40 nm or (b) 65 nm at remanent state after saturating at 5000 Oe. Two distinct types of magnetic domain configurations were observed in the MFM images as shown Figure 4: vortex and onion states. Since the vortex state is a closed magnetic flux, magnetic flux do not appear in a ring element. Therefore, there is no magnetic flux image observed in elements C1, C2, C3, and C4 in Figure 4(b). It was found in this study that the

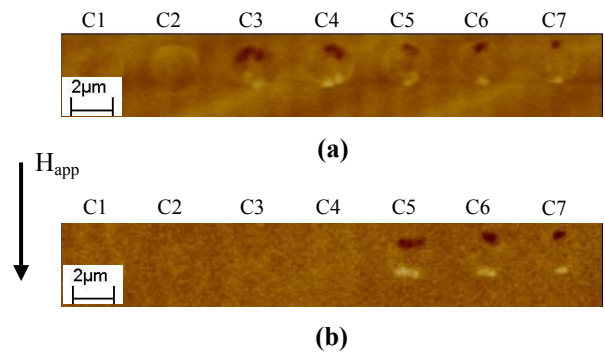


Figure 4. MFM images of 40 nm (a) and 60 nm thick (b) permalloy ring elements with an outer diameter of 2.0 μm at remanent states after saturating at 5000 Oe.

magnetization state of a ring element is strongly dependent on the ratio of the inner and outer diameter ($R_{i/O}$) and the thickness. As shown in Figure 4, the onion state is stable in 40 nm thick ring elements with $R_{i/O}$ greater than 0.4, otherwise the vortex state is stable. On the contrary, for the 65 nm thick ring element, the onion

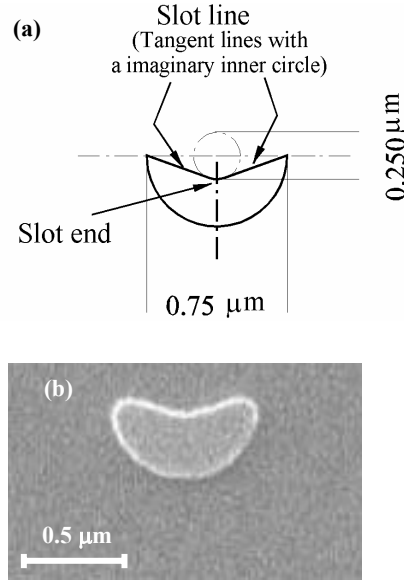


Figure 5. (a) Definition and dimensions of PM element and (b) SEM image of 40 nm thick permalloy PM element.

state is stable for $R_{I/O}$ greater than 0.6, while the vortex state is favorable for $R_{I/O}$ less than 0.5. This can be explained by the exchange and magnetostatic energies. Magnetic flux produced at the HTH domain wall increases when decreasing the $R_{I/O}$ (increasing the ring width) and increasing the ring thickness, resulting in an increase in the magnetostatic energy of the ring element. Consequently, an onion state becomes unstable with decreasing $R_{I/O}$ and increasing thickness of the ring.

Interestingly, it was found that the location of a HTH domain wall of an onion state is inconsistent between elements. It is attributed to physical defects existing in ring elements. These defects are energetically favorable sites for the HTH domain walls. It was observed that the effect of physical defects on the onion state magnetization configuration is more serious as the $R_{I/O}$ decreases. An unrepeatable switching process is expected in an onion state, which will result in a wide SFD between elements.

2.3 Pac-man element

Magnetization configuration and SFD of PM elements were studied. This magnetic element is shaped as a ring with an open slot toward the center, as described in Figure 5 (a). It has a round slot end having two-slot lines tangent to a small imaginary circle (0.25 μm) at the element center. SEM images of the PM element is shown in Figure 5 (b). AFM and MFM images of an array of permalloy PM elements at as-patterned state are shown in Figure 6 (a) for 40 nm thick elements and (b) for 65 nm.

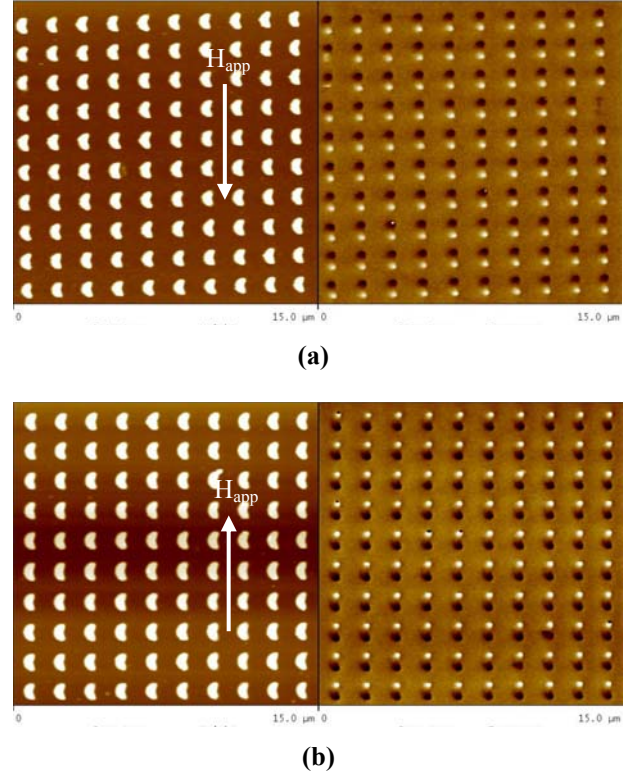
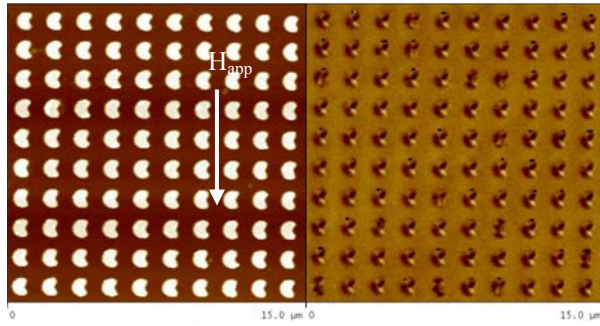


Figure 6. AFM/MFM images of an array of 40 nm (a) and 60 nm (b) permalloy PM elements.

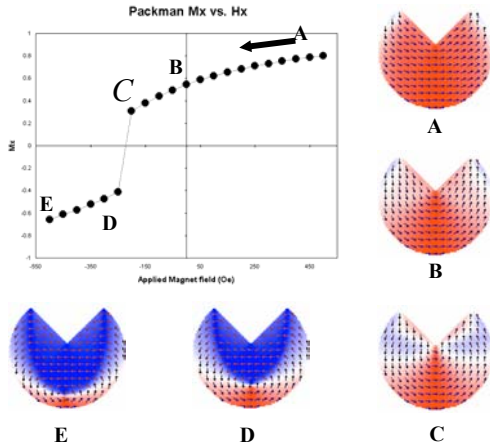
50 Oe of a magnetic field was applied during deposition to induce an anisotropy in the element. Single domain configurations are observed by MFM images. However, a single domain state is unstable for the modified PM element with a sharp slot end shape as shown in Figure 7 (a). Instead, a bi-domain state is favorable to exist. Micromagnetic computer simulation using the Landau-Lifshitz-Gilbert equation confirmed the reversal process occurs by a vortex core movement as shown in Figure 7 (b). An abrupt drop in the magnetization value corresponds to the nucleation of a vortex core. Figure 7 (b) shows the domain configuration of a modified PM element is not a bi-domain state at remanent state. This is not in agreement with our experimental results. It may be attributed to the simulation performed at 0 K.

Note the modified PM element shown in Figure 7 has an angle of 90° between slot lines, but the PM elements in Figure 5 and 6 have 180° . The angle dependence of magnetic domain configuration for PM elements is described elsewhere [22]. Since the magnetic switching process by a vortex core movement is slower than that occurred by a coherent rotation, the modified PM element is not the desired shape for MRAM applications.

High selectivity is expected in the PM element with a round slot end as compared to conversational hexagonal



(a)



(b)

Figure 7. (a) AFM/MFM images of as-patterned array of 40 nm thick modified permalloy PM element. (b) Micromagnetic computer simulation results of the modified PM element using LLG equation. Reversal process is driven by the vortex core movement.

element because the domain configuration of the PM element resembles a C-domain state [23].

Finally, we confirmed that the SFD of an array of the PM elements is narrower than the hexagonal and rectangular elements with the overall same dimension. These results are described elsewhere [22].

3. Summary

Various shapes of magnetic elements were studied for magnetization configuration and switching behaviors for MRAM applications. An unrepeatable switching process was observed in rectangular elements, and a wide SFD of an array of hexagonal elements is attributed to small end shape variations. Ring elements with a narrow width show a stable onion state, but a non-uniform magnetization configuration was observed due to the small lateral roughness. A PM element proposed in this study possesses a single domain configuration and a narrower SFD as compared to the linear elements,

rectangle and hexagon, with the same overall dimensions. The C-domain configuration of the PM element potentially provides a high selectivity with an orthogonal conducting wire configuration. We conclude the PM element has the most potential for a magnetic memory element in future MRAM devices.

4. Acknowledgement

A part of this research was supported by ONR under contract number N00014-02-1-0991.

5. References

- [1] G. R. Fox, F. Chu, and T. Davenport, "Current and future ferroelectric nonvolatile memory technology," *J. Vac. Sci. Tech. B.* **19**, Sept. 2001, pp. 1967-1971
- [2] Uong Chon, Jeong Seob Shim, and Hyun M. Jang, "Ferroelectric properties and crystal structure of praseodymium-modified bismuth titanate," *J. Appl. Phys.* **93**, April 2003, pp. 4769-4775
- [3] M. Gill, T. Lowrey, J. Park, "Ovonic unified memory- a high -performance nonvolatile memory technology for stand-alone memory and embedded applications," 2002 ISSCC Digest of Technical Papers, Feb 2002, pp. 202
- [4] Kazuya Nakayama, Kazuhiko Kojima, Yutaka Imai, Toshihiko Kasai, Sanae Fukushima, Akio Kitagawa, Minoru Kumeda, Yoshio Kakimoto, and Masakuni Suzuki, "Nonvolatile Memory Based on Phase Change in Se-Sb-Te Glass," *Jpn. J. Appl. Phys., Part 1* **42**, Feb. 2003, pp. 404-408
- [5] S. S. P. Parkin, K. P. Roche, M. G. Samant, P. M. Rice, R. B. Beyers, R. E. Scheuerlein, E. J. O'Sullivan, S. L. Brown, J. Bucchigano, D. W. Abraham, Y. Lu, M. Rooks, P. L. Trouilloud, R. A. Wanner, and W. Ghallagher, "Exchange-biased magnetic tunnel junctions and application to nonvolatile magnetic random access memory (invited)" *J. Appl. Phys.* **85**, April 1999, pp. 5828-5833
- [6] M. Durlam, P. Naji, A. Omair, M. DeHerrera, J. Calder, J. M. Slaughter, B. Engel, N. Rizzo, G. Grynkeiwich, B. Butcher, C. Tracy, K. Smith, K. Kyler, J. Ren, J. Molla, B. Feil, R. Williams, and S. Tehrani, "A low power 1Mbit MRAM based on 1T1MTJ bit cell integrated with Copper Interconnects," 2002 VLSI Symposia on Technology, June 2002, C12p4
- [7] B. Engel, N. Rizzo, J. Janesky, J. M. Slaughter, M. Durlam, P. Naji, G. Grynkeiwich, and S. Tehrani, "Prototype 256-kbit Magnetoresistive Random Access Memory (MRAM)," 2001 Non-volatile Memory Workshop at UCSD, CA, Sep. 2001
- [8] Zongzhi Zhang, S. Cardoso, P. P. Freitas, X. Batlle, P. Wei, N. Barradas, and J. C. Soares, "40% tunneling magnetoresistance after anneal at 380°C for tunnel junctions with iron-oxide interface layers," *J. Appl. Phys.* **89**, June 2001, pp. 6665-6667
- [9] Youfeng Zheng and Jian-Gang Zhu, "Switching field variation in patterned submicron magnetic film elements," *J. Appl. Phys.* **81**, April 1997, pp. 5471-5473
- [10] X. Portier and A. K. Petford-Long, "The formation of 360° domain walls in magnetic tunnel junction elements," *Appl. Phys. Lett.* **76**, Feb. 2000, pp. 754-756

- [11] J. Shi, S. Tehrani, T. Zhu, Y. F. Zheng, and J. G. Zhu, "Magnetization vortices and anomalous switching in patterned NiFeCo submicron arrays," *Appl. Phys. Lett.* **74**, April 1999, pp. 2525-2527
- [12] Jim Daughton, "MRAM: Status and Opportunities," 2001 Non-volatile Memory Workshop at UCSD, CA, Sep. 2001
- [13] R. P. Cowburn, D. K. Koltsov, A. O. Adeyeye, and M. E. Welland, "Lateral interface anisotropy in nanomagnets," *J. Appl. Phys.* **87**, May 2000, pp. 7067-7069
- [14] J. M. Ryan, A. C. F. Hoole, and A. N. Broers, "A study of the effect of ultrasonic agitation during development of poly(methylmethacrylate) for ultrahigh resolution electron-beam lithography," *J. Vac. Sci. Technol. B* **13**, Nov. 1995, pp. 3035-3039
- [15] J. Gadbois, J. G. Zhu, W. Vavra and A. Hurst, "The effect of end and edge shape on the performance of pseudo-spin valve memories," *IEEE Trans. Magn.* **34**, July 1998, pp. 1066-1068
- [16]
- [17] R. P. Cowburn, D. K. Koltsov, A. O. Adeyeye, M. E. Welland, and D. M. Tricker, "Single-Domain Circular Nanomagnets," *Phys. Rev. Lett.* **83**, August 1999, pp. 1042-1045
- [18] M. Schneider, H. Hoffmann, S. Otto, Th. Haug, and J. Zweck, "Stability of magnetic vortices in flat submicron permalloy cylinders," *J. Appl. Phys.* **92**, August 2002, pp. 1466-1472
- [19] Jian-Gang Zhu, Youfeng Zheng, and Gary A. Prinz, "Ultrahigh density vertical magnetoresistive random access memory (invited)," *J. Appl. Phys.* **87**, May 2000, pp. 6668-6673
- [20] M. Kläui, C. A. F. Vaz, J. Rothman, J. A. C. Bland, W. Wernsdorfer, G. Faini, and E. Cambril, "Domain Wall Pinning in Narrow Ferromagnetic Ring Structures Probed by Magnetoresistance Measurements," *Phys. Rev. Lett.* **90**, March 2003, pp. 97202-97205
- [21] N. Kikuchi, S. Okamoto, O. Kitakami, Y. Shimada, S. G. Kim, Y. Otani, and K. Fukamichi, "Vertical Magnetization Process in Sub-Micron Permalloy Dots," *IEEE Trans. Magn.* **37**, July 2001, pp. 2082-2084
- [22] J. Rothman, M. Kläui, L. Lopez-Diaz, C. A. F. Vaz, A. Bleloch, J. A. C. Bland, Z. Cui, and R. Speaks, "Observation of a Bi-Domain State and Nucleation Free Switching in Mesoscopic Ring Magnets," *Phys. Rev. Lett.* **86**, Feb. 2001, pp. 1098-1101 (2001)
- [23] M.H. Park, Y.K. Hong, S.H. Gee, D. W. Erickson, and B.C. Choi, "Magnetization configuration and switching behavior of newly shaped submicron NiFe elements: Pac-man shape," submitted to *Appl. Phys. Lett.* 2003.
- [24] A. S. Arrott, "High Selectivity for Magnetic Random Access Memory," presented at 46th MMM Conf., paper number EC-11, Seattle, Nov. 2001, pp. 18